Cross-network coupling of neural oscillations in the dynamic pain connectome reflects chronic neuropathic pain in multiple sclerosis

Junseok A. Kim[a,b], Rachael L. Bosma[a], Kasey S. Hemington[a,b], Anton Rogachov[a,b], Natalie R. Osborne[a,b], Joshua C. Cheng[a,b], Jiwon Oh[c], Benjamin T. Dunkley[d,e], Karen D. Davis[a,b,f,*]

[a] Division of Brain, Imaging and Behaviour, Krembil Brain Institute, Krembil Research Institute, University Health Network, M5T2S8, Toronto, Canada
[b] Institute of Medical Science, Faculty of Medicine, University of Toronto, M5S1A8, Toronto, Canada
[c] Division of Neurology, Department of Medicine, St. Michael's Hospital, M5B1W8, Toronto, Canada
[d] Department of Medical Imaging, University of Toronto, M5T1W7, Toronto, Canada
[e] Neurosciences & Mental Health Program, The Hospital for Sick Children Research Institute, M5G0A4, Toronto, Canada
[f] Department of Surgery, University of Toronto, M5T1P5, Toronto, Canada

ARTICLE INFO

ABSTRACT

Sensory perceptions are coded by complex neural dynamics of regional communication in the brain. Thus, sensory abnormalities such as chronic pain may occur when neural dynamics go awry. Previous studies of cross-network dynamic functional connectivity in chronic pain identified abnormalities but were based on functional MRI which only captures slow temporal features. Here we conducted a magnetoencephalography (MEG) study to investigate fine temporal dynamics of aberrant cross-regional and cross-network communication of the dynamic pain connectome in patients with chronic pain. We also introduced a novel measure, dynamic functional coupling, to quantify the variability of brain communication. The study was performed in 33 people who had chronic pain associated with multiple sclerosis and 30 healthy controls. We found that patients with chronic pain exhibited abnormalities in cross-network functional coupling across multiple frequency bands (theta, alpha, beta, gamma), between the salience network and 3 other networks: the ascending nociceptive pathway, descending anti-nociceptive pathway, and the default mode network. However, these cross-network abnormalities involved different frequency bands in patients with neuropathic versus non-neuropathic chronic pain. Furthermore, cross-network abnormalities were linked to pain severity and pain interference. Our findings implicate broadband cross-network abnormalities as hallmark features of chronic pain in multiple sclerosis.

1. Introduction

Neuropathic pain is a type of chronic pain defined as "pain caused by a lesion or disease affecting the somatosensory system" (Jensen et al., 2011). Neuropathic pain is present across a variety of neurological conditions, but the key brain aberrations that could serve as hallmarks of neuropathic pain compared to non-neuropathic types of pain are unknown. We and others have previously used functional magnetic resonance imaging (fMRI) to identify regional and cross-regional static and dynamic connectivity abnormalities in neuropathic pain (Cauda et al., 2009b, 2009a, 2010; Bosma et al., 2018b, 2018a; Rogachov et al., 2019), particularly within the default mode network and salience networks (DMN, SN) of the dynamic pain connectome (Kucyi and Davis, 2015, 2017). These studies demonstrate that the co-

ordination of brain dynamics on a network level is essential to pain processing and thus mismatches of brain dynamics may underlie chronic pain conditions. To detect aberrations in fine temporal brain dynamics in neuropathic pain, we and others have utilized the millisecond temporal resolution of electroencephalography (EEG) and magnetoencephalography (MEG) to measure oscillations in the brain. These oscillations provide useful information about the underlying neural mechanisms (Buzsaki, 2006) because neural oscillations are crucial for functional segregation and integration within the brain and specific oscillatory activity (i.e. activity in functional bands) have been associated with specific functions in the brain (Buzsáki and Draguhn, 2004). Using M/EEG, neuropathic pain showed reduction of the peak alpha frequency (Sarnthein et al., 2006; Stern et al., 2006; de Vries et al., 2013; Kim et al., 2019). These M/EEG studies and the

previously mentioned fMRI studies demonstrated possible common brain abnormalities underlying neuropathic pain and showed that the mechanism may be different in non-neuropathic pain.

Multiple Sclerosis (MS) is an autoimmune, inflammatory disease of the central nervous system which lead to deficits, including motor and cognitive deficits, sensory loss and chronic pain (Goldenberg, 2012). Majority of people living with MS suffer from chronic pain, including neuropathic and non-neuropathic pain, which makes MS a candidate disease model to study both neuropathic and non-neuropathic pain (O'Connor et al., 2008). Previous works using MEG and fMRI have already shown abnormalities in regional spectral power as well as functional connectivity related to pain levels and pain interference in MS patients with neuropathic pain but not with non-neuropathic pain (Bosma et al., 2018a; Kim et al., 2019). These abnormalities were observed within regions of the dynamic pain connectome consisting of the DMN, SN, ascending nociceptive pathway (Asc) and the descending anti-nociceptive pathway (Desc) (Kucyi and Davis, 2015, 2017).

To understand how inter-regional communication in the brain contributes to chronic pain, it is important to assess three aspects of inter-regional activity: 1) The contribution of abnormalities within a brain region (i.e., regional activity) to failures in cross-regional communication. 2) The frequency band(s) contributing to cross-regional communication failures. 3) The dynamics of cross-regional communication failure in terms of dynamic functional coupling (FCp) (e.g. amplitude and phase-based), given the recent recognition of the importance of brain dynamics in chronic pain (Kucyi and Davis, 2015; Davis, 2019).

Here we interrogated inter-regional communication failures as a potential mechanism underlying chronic pain in MS and examined how these abnormalities may be related to neuropathic and non-neuropathic types of pain. Abnormalities in inter-regional oscillatory activity, such as thalamocortical dysrhythmia, have previously been theorized to lead to sensory deficits including neuropathic pain (Llinas et al., 1999). However, only a scant number of studies have used EEG to investigate the link between neuropathic pain and abnormalities in inter-regional oscillatory activity (Sarnthein and Jeanmonod, 2008; Walton et al., 2010). As such, we aimed to determine whether inter-regional abnormalities between regions of the brain associated with pain processing are associated with specific types of pain (i.e. neuropathic and non-neuropathic pain) using two distinct measure of MEG functional connectivity: amplitude and phase coupling to investigate different mechanistic aspects about the underlying neural circuitry (Siegel et al., 2012). We also linked our neural dynamics findings to measures of pain and pain interference. Specifically, we examined state pain (pain on the day of the scan) and trait pain (average pain over the week) because they have been shown to have distinct representations based on cross-network dynamic functional connectivity in patients with neuropathic pain (Bosma et al., 2018b; Davis and Cheng, 2019). Thus, the study aims to determine: 1) the location and frequency of cross-regional abnormalities, 2) whether these abnormalities present differently in neuropathic pain, and 3) whether these brain abnormalities are related to pain-specific measures including trait pain, state pain, and pain interference.

2. Materials and methods

2.1. Participants

Participants consisted of 33 patients diagnosed with MS (12 males, 21 females, mean ± S.D. age 39 ± 10 years) and 30 healthy controls (11 males, 19 females, mean ± S.D. age 35 ± 9 years) with no significance difference in age ($p = 0.09$) or sex (Fisher's exact $p = 1$) between the groups. All participants provided informed written consent to the procedures approved by the research ethics boards of the University Heath Network and St. Michael's Hospital. The patients with MS were recruited from the MS clinic at St. Michael's Hospital with the

following inclusion criteria: 1) diagnosis of MS evaluated by staff neurologists at St. Michael's Hospital according to the 2010 McDonald criteria, 2) able to ambulate without assistance, 3) free of any pain condition that was clinically deemed to be unrelated to MS, and 4) no contraindications for MRI. The inclusion criteria for the healthy control group were: 1) no prior history of chronic pain or current experience of pain on a regular basis, 2) free of metabolic, psychiatric or neurologic conditions, 3) no history of major surgery due to a physiological condition, and 4) no contraindications for MRI.

2.2. Clinical assessment and questionnaires

Clinical information obtained from the MS clinic included: disease duration, disease sub-type, and global neurological disability as measured by the Expanded Disability Status Scale (EDSS) score (Kurtzke, 1983). The EDSS is a neurological disability score in MS that ranges from 0 to 10, with increasing values reflecting greater neurological disability. Those in the MS group also completed the painDETECT questionnaire (Freynhagen et al., 2006) to distinguish those with a component of neuropathic pain (scores ≥13) from those with only non-neuropathic pain (scores <13). PainDETECT possible scores range from 0–38; scores 19–38 indicate a definitive neuropathic pain, scores 13–18 indicate a probable component of neuropathic pain (i.e., mixed-neuropathic pain and non-neuropathic pain), and scores 0–12 indicate non-neuropathic pain. Trait pain (average pain level over the last week) and state pain (pain level right now), were measured using the Brief Pain Inventory (BPI) that had a ranges from 0–10 (0 = no pain 10 = worst pain imaginable) (Turk et al., 2003; Dworkin et al., 2005; Osborne et al., 2006). Pain interference was also measured using the BPI (0–10, 0 = no interference,10 = complete interference) with items such as general activity, mood, walking ability, normal work, relations with other people, sleep, and enjoyment of life. Pain quality was assessed using the McGill Pain Questionnaire (Melzack and Torgerson, 1971; Melzack, 1975). The Hospital Anxiety and Depression Scale (HADS) (Zigmond and Snaith, 1983) was used to assess non-physical symptoms of anxiety and depression with ratings of at least 8 considered clinically significant.

2.3. MEG acquisition

A 5 min resting-state MEG scan was collected with the 306 channel Elekta Neuromag TRIUX system with a 1000 Hz sampling rate and recording DC bandpass of 330 Hz. Each participant was deemed free of any metallic objects or traces of metal from make up or hair products before they were placed inside the magnetically shielded room in an upright position in the scanner. Fiducial reference points at the nasion, right and left preauricular positions as well as 5 head position coils were marked and confirmed using an electrical head position co-ordinate system for co-registration and motion correction purposes. Participants underwent an 'eyes-open' resting state scan with their eyes fixated on a crosshair with the lights turned off during the 5 min. The tSSS algorithm in the MaxFilter program was used to correct for various artifacts. For purposes of co-registration, a 3T MRI (GE Medical Systems, Chicago, IL) of the brain was used to acquire high resolution T1 anatomical images for each participant ($1 \times 1 \times 1$ mm^3 voxels, matrix = 256×256, FOV = 25.6, flip angle 15°, 180 axial slices, repetition time = 7.8 s, echo time = 3 ms, inversion time = 450 ms). MEG data for each participant was co-registered to their anatomical MRI scan using the fiducial points obtained before the MEG session for source reconstruction/inverse solution.

2.4. MEG data preprocessing and beamforming

Resting state data processing was performed using the MATLAB-based program FieldTrip (http://www.fieldtriptoolbox.org/). A bandpass filter was applied between 1–150 Hz and a notch filter was applied

at 60 Hz and 120 Hz. We used the results of an independent components analysis and visual inspection to remove components from the resting state time series data that were likely to reflect artifacts induced by respiration and eye-blinks artifacts. The fiducial points obtained before the scan were identified on each individual's MRI and used to register each individual's high resolution anatomical image to their resting state MEG data. The forward model was constructed using a single-shell morel.

Construction of 'virtual sensors' were performed on previously defined regions of interest (ROIs) using the atlas-guided beamforming method (Hillebrand et al., 2012). Briefly, using Linearly Constrained Minimum Variance beamformer (Van Veen et al., 1997), each time-series was reconstructed for each ROI at the center of mass. Beamforming is used to obtain signals of interest that originate from the defined ROI while optimally suppressing the signals from other sources. To do this, a weighting vector is calculated for each source location in the brain and is applied to the physical sensor's time course. The resultant time-series are summated and give a reconstructed signal for the specified source location over time.

2.5. Regions of interest

The ROIs within key components of the dynamic pain connectome were selected for the atlas-guided beamforming. The ROIs chosen based on our previous MEG study (Kim et al., 2019) and the co-ordinates are provided in MNI space: 1) Asc: left primary somatosensory cortex (S1) (-34, -30, 54), right S1 (34, -28, 54), left secondary somatosensory cortex (S2) (-60, -30, 20), right S2 (60, -22, 18), left posterior insula (-34, -20, 18), right posterior insula (34, -20, 18), left thalamus (-12, -18, 8), right thalamus (12, -18, 8); 2) SN: right temporoparietal junction (TPJ) (50, -32, 28), right anterior insula (34, 18, 4), mid cingulate cortex (MCC) (2, 12, 34), right dorsolateral prefrontal cortex (dlPFC) (34, 46, 22); 3) DMN: posterior cingulate cortex (PCC) (-2, -46, 28), and medial prefrontal cortex (mPFC) (-2, 50, 2), 4) Desc: subgenual anterior cingulate cortex (sgACC) (4, 26 -8).

2.6. Functional coupling calculation

MEG metrics which can be used to determine network level dynamics include amplitude envelope correlation (Liu et al., 2010) and weighted phase lag index (wPLI) (Vinck et al., 2011). In amplitude coupling, correlations of band-limited amplitude envelope are calculated between time-series extracted from to nodes of interest. The wPLI is a measure that shows the amount of phase synchronization between two nodes of interest by assessing if there are consistent leads or lags in the phase difference of the two nodes. Amplitude and phased measures of coupling are believed to reflect different underlying neural mechanisms in network interaction (Siegel et al., 2012) thus assessing these two metrics allows for different interpretations of network interactions. The FCp values were calculated across each pair of ROIs using the mathematical formula for amplitude envelope correlation and weighted phase lag index. For each time point in the resting state time-series, the instantaneous phase and amplitude was calculated with the Hilbert Transform. For the Hilbert Transform, a finite impulse response filter was used to divide the time-series data into previously defined frequency bands: theta (4–8 Hz), alpha (8–13 Hz), beta (13–30 Hz), low gamma (30–60 Hz), and high gamma (60–150 Hz). In order to remove linear dependencies from the signal and control for source leakage, orthogonalization was applied to the time-series in each ROI using the ROI-nets toolbox (Colclough et al., 2015). Orthogonalization takes a set of non-orthogonal independent functions and creates an orthogonal relationship between them. In amplitude envelope correlation this process removes false coupling between two different sources which may have signals originating from the same source. For each participant, their resting state scan was divided into 10 s epochs, and the first and last 10 s of the scan were removed, resulting in 28 epochs of data.

Static FCp is used to determine the average strength of interaction between two brain regions. Here, we determined static and dynamic FCp values for each frequency band in each participant as follows: We calculated a single FCp value to represent static FCp as the epoch average over the 28 epochs, where epoch averages were determined by averaging FCp values over the 10 s within an epoch. Our novel measure of dynamic FCp was used to determine the dynamic fluctuation of the interaction strength between two brain regions. To do so, we calculated a single value to represent dynamic FCp in each participant based on the standard deviation of FCp values across the 28 10 s epochs.

2.7. Statistical testing

Group differences in amplitude envelope correlation and wPLI were analyzed using two-tailed Student's t-test between the MS groups and the respective healthy control matched groups. Multiple comparison corrections were performed using false discovery rate with the Benjamini-Hochberg method (Benjamini and Hochberg, 1995) at $p = 0.05$. In one of the sub-analyses, the top 10% pairs of nodes, ordered by strength of both static and dynamic FCp, were extracted in the healthy control group for each functional band. Static and dynamic FCp values from these nodes were then compared against the MS group using Student's t-test. Group differences for categorical data (e.g., sex) were calculated using Fisher's exact test. Correlation analyses between state pain, trait pain and pain interference with amplitude envelope correlation and wPLI were performed using Spearman's correlation with false discovery rate for multiple comparison corrections.

3. Results

3.1. Demographics

Demographic information for the healthy control and MS groups are summarized in Table 1. The healthy control and MS groups were not statistically different in age ($p = 0.09$) or sex (Fisher's exact $p = 1$). However, the MS groups had significantly higher anxiety ($p = 0.00003$) and depression ($p = 0.00009$). In the entire MS group, the average trait pain intensity was 3.7 ± 2.9 (mean ± S.D.), the average state pain intensity was 2.5 ± 2.7 (mean ± S.D.), the average pain interference was 3.2 ± 2.8 (mean ± S.D.) and the average PainDETECT score was 12.3 ± 8.3 (mean ± S.D.). Within the NP group, the average trait pain intensity was 5 ± 2.8 (mean ± S.D.), the average state pain intensity was 3.4 ± 3 (mean ± S.D.), the average pain interference was 4.8 ± 2.7 (mean ± S.D.) and the average PainDETECT score was 20 ± 3.9 (mean ± S.D.). Within the NNP group, the average trait pain intensity was 2.5 ± 2.4 (mean ± S.D.), the average state pain intensity was 1.7 ± 2 (mean ± S.D.), the average pain interference was 1.7 ± 2 (mean ± S.D.) and the average PainDETECT score was 5 ± 3 (mean ± S.D.). In terms of chronic pain quality, patients in the NP group most often described their pain as "Burning" (11/16), "Tiring" (9/16) or "Shooting", "Radiating" and "Numb" (8/16). In contrast, patients in the NNP group described their pain most often as "Aching" or "Annoying" (9/17) and "Sharp" or "Tingling" (7/17). In both the NP and NNP groups, the location of pain was reported to be bilateral by 23/33 people and the specific location of pain was most often reported to be in the upper body (17/33), lower body (22/33), back (18/33), or head/face (12/33) area. Specifically, within the NP group, pain was reported by 14/16 to involve multiple regions and for 13/16 people the pain was bilateral. In the NNP group, 10/17 people reported pain in multiple regions and 10/17 had bilateral pain. Between the subgroups, the neuropathic pain and non-neuropathic groups were not different in sex (Fisher's exact $p = 1$) and state pain ($p = 0.06$) however the NP group had significantly higher age ($p = 0.003$), trait pain ($p = 0.01$), depression ($p = 0.006$), anxiety ($p = 0.01$), average pain interference ($p = 0.0006$) and EDSS ($p = 0.001$).

Table 1
Demographics and characteristics of HC and MS groups.

| | Groups | | MS Subgroups | |
	HC	MS	MS (NP)	MS (NNP)
N	30	33	16	17
Age (years)	35 ± 9	39 ± 10	44 ± 9	35 ± 8**
Sex	11 M 19W	12 M 21W	6 M 10W	6 M 11W
Years since MS onset	N/A	10 ± 7	12 ± 9	8 ± 5
Average EDSS (/10)	N/A	2 ± 2	3 ± 2	1 ± 1**
Type of MS	N/A	28 RR 1 RIS 4 SPMS	12 RR 4 SPMS	16 RR 1 RIS
Trait Pain (/10)	N/A	3.7 ± 2.9	5 ± 2.8	2.5 ± 2.4**
State Pain (/10)	N/A	2.5 ± 2.7	3.4 ± 3	1.7 ± 2
Avg. Pain interference (/10)	N/A	3.2 ± 2.8	4.8 ± 2.7	1.7 ± 2**
PainDetect	N/A	12.3 ± 8.3	20 ± 3.9	5 ± 3**
HADS Depression (/21)	3 ± 3	8 ± 5*	10 ± 5	5 ± 5**
HADS Anxiety (/21)	3 ± 3	7 ± 5*	9 ± 4	5 ± 4**

EDSS, Expanded Disability and Severity Scale; HADS, Hospital Anxiety and Depression Scale; HC, Healthy Control; MS, Multiple Sclerosis; NP, Neuropathic pain; NNP, Non-neuropathic pain; RIS, radiologically isolated syndrome; RR, Relapsing Remitting; SPMS, secondary progressive multiple sclerosis.
All means are provided with S.D.
  * Indicates significant differences at $p < 0.05$ between the HC and MS groups.
  ** Indicates significant subgroup differences at $p < 0.05$ between the MS (NP) and MS (NNP) subgroups.

3.2. Static functional coupling: widespread within- and cross-network abnormalities in alpha, beta and gamma bands

Static functional coupling across all nodes and bands for the heathy control and multiple sclerosis groups are shown in Supplementary Figures 1 and 2. Compared to the healthy control group, the chronic pain group exhibited abnormal static functional coupling within and between pain connectome networks within multiple frequency bands. A summary of these findings is shown in Fig. 1 and examples of individual nodes are shown in Fig. 2.

The static amplitude envelope correlation of nodes in the ascending nociceptive pathway showed broadband attenuation. Specifically, the chronic pain group exhibited lower static amplitude envelope correlation between within network inter-hemispheric nodes of the posterior insula cortices within the alpha ($p = 0.008$), beta ($p = 0.003$), and low gamma ($p = 0.0001$) bands, as well as between left and the right thalamus ($p = 0.017$), left thalamus and the right posterior insula ($p = 0.0005$ (low gamma)), right thalamus and left S1 ($p = 0.02$ (beta), $p = 0.01$ (low gamma)), right thalamus and left S2 ($p = 0.007$) right thalamus and left posterior insula ($p = 0.01$ (beta), $p = 0.002$ (low gamma)), left S2 and right posterior insula ($p = 0.02$), left S2 and right S2 ($p = 0.002$) and right S2 and left posterior insula ($p = 0.004$), within the beta and low gamma bands. There was also abnormal alpha and beta band static amplitude envelope correlations between nodes of the SN and Desc (right anterior insula-subgenual ACC, $p = 0.007$ (alpha), $p = 0.007$ (beta)) (Fig. 2a). Furthermore, cross-network alpha, beta, and low gamma static amplitude envelope correlations were also lower in patients with chronic pain compared to healthy controls between SN and Asc (right TPJ-left posterior insula, $p = 0.009$) (Fig. 2b) and SN and DMN (right anterior insula-mPFC, $p = 0.03$) (right anterior insula-PCC, $p = 0.01$ (alpha, beta)).

3.3. Dynamic functional coupling: within- and cross-network abnormalities in theta and alpha bands

The patients with multiple sclerosis chronic pain exhibited abnormal within- and cross-network dynamic functional coupling amplitude envelope correlation (Fig. 3). The multiple sclerosis chronic pain group had attenuated dynamic amplitude envelope correlation between the Asc and the SN (left thalamus-right TPJ, $p = 0.015$ and left posterior insula-right TPJ $p = 0.01$) in the theta band (Fig. 3a) compared to healthy controls. However, within the theta band, there was also increased dynamic amplitude envelope correlation in the multiple sclerosis group between other areas of the Asc and SN (right S2-right TPJ, $p = 0.009$) and within the SN (right TPJ-MCC) ($p = 0.009$). The

alpha band also showed reductions in dynamic amplitude envelope correlation in the chronic pain group. These attenuations were found within the ascending nociceptive pathway (right S1-right posterior insula, $p = 0.007$), and between the DMN and Asc (left thalamus-PCC, $p = 0.007$) and SN (right anterior insula-PCC, $p = 0.006$) in the alpha band (Fig. 3b). Dynamic functional coupling findings for the healthy control and multiple sclerosis groups across all nodes and bands are summarized in Fig. 1 and Supplementary Figures 3 and 4.

3.4. The top 10% of normally highly connected nodes exhibit abnormal cross-network alpha dynamic functional coupling in chronic pain

We conducted a sub-analysis to focus on the areas that normally have the most robust functional coupling. To do this, we first extracted the top 10% of static and dynamic functional coupling values in all functional bands from the healthy control group data (Supplementary Table 1). We then compared the functional coupling values at these locations and frequencies to those in the chronic pain group. This approach identified attenuated alpha band dynamic amplitude coupling within the ascending nociceptive pathway (right S1- posterior insula, $p = 0.007$), and also cross-network attenuations between the DMN and the SN (PCC-right anterior insula, $p = 0.007$) and Asc (PCC-left thalamus, $p = 0.007$) in the chronic pain group.

3.5. Subgroup analysis: abnormal functional coupling in neuropathic pain

In the subgroup analysis, patients with neuropathic pain exhibited static functional coupling (amplitude envelope and wPLI) abnormalities in the theta, alpha and low gamma bands (Fig. 1 Supplementary Table 2). Specifically, in the patients with neuropathic pain we identified abnormal within-network static amplitude envelope correlation and static wPLI inter-hemispherically between nodes of the ascending nociceptive pathway (right thalamus-left S1, $p = 0.012$) (right posterior insula-left S1, $p = 0.014$) in the alpha band and within the SN (right TPJ-MCC, $p = 0.007$, Fig. 4a) in the low gamma band. Also, in the neuropathic pain group, there was reduced cross-network static amplitude envelope correlation between nodes of SN-Desc (right anterior insula-subgenual ACC) ($p = 0.008$) in the alpha (Fig. 4a) and ($p = 0.004$) beta bands. Lastly, abnormal static wPLI was observed between cross-network nodes of Asc-SN (right thalamus-right TPJ, $p = 0.005$) (left S2-MCC, $p = 0.009$), Asc-Desc (right S1-subgenual ACC, $p = 0.001$) and SN-DMN (right TPJ-mPFC, $p = 0.0008$) in the theta and alpha bands.

Both neuropathic and non-neuropathic groups (see sections below for non-neuropathic pain groups) had widespread cross-network
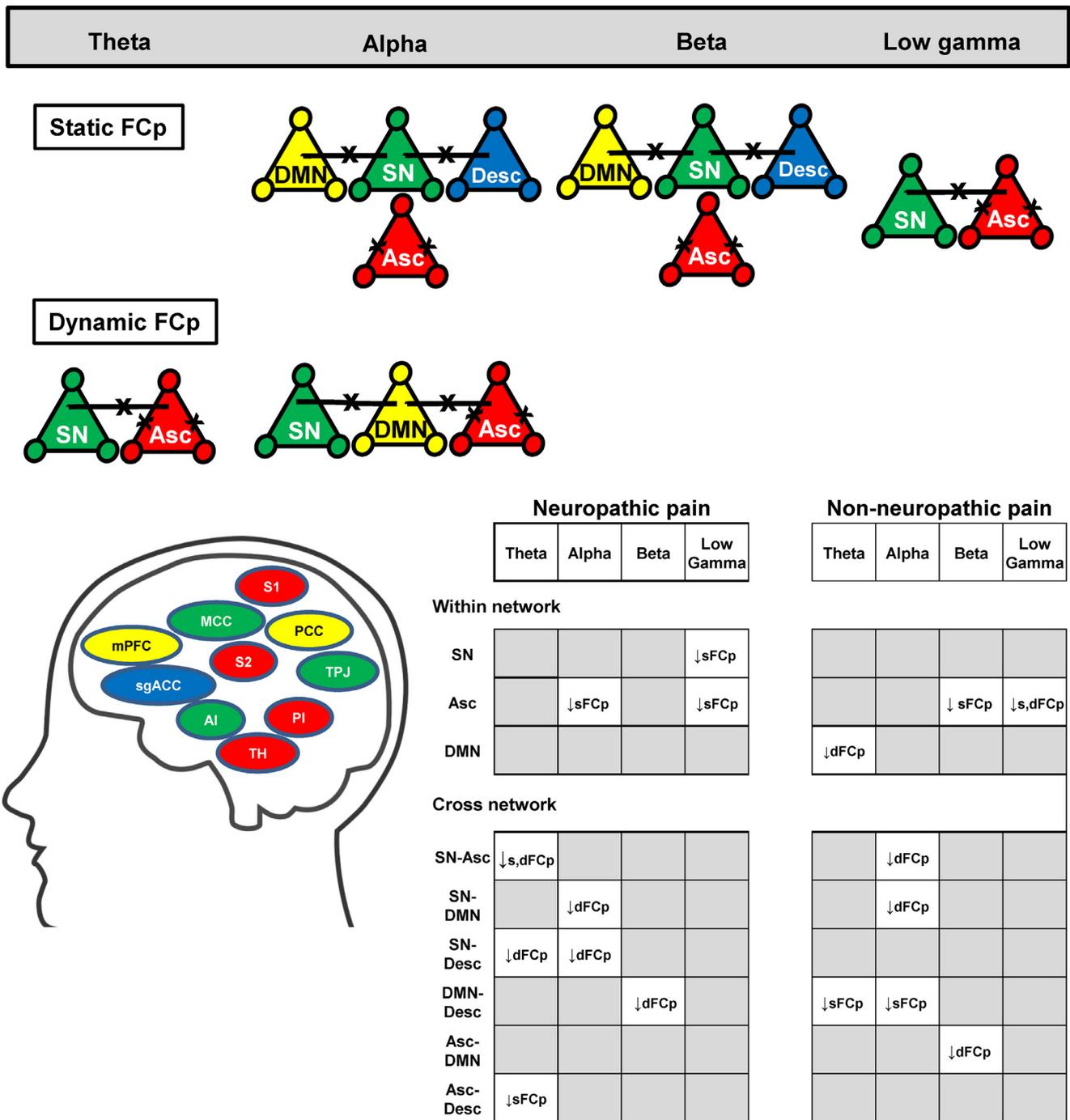
Fig. 1. Summary figure showing within- and cross- network abnormalities in chronic pain.
Static functional coupling abnormalities in alpha, beta, and low gamma and dynamic functional coupling abnormalities in theta, alpha, beta and low gamma are depicted in the figure where the x marks abnormality within or between networks. The within- and cross network abnormalities in the sub group analysis are also shown as a table in the figure. Both static (sFCp) and dynamic (dFCp) functional coupling abnormalities in theta, alpha, beta and low gamma are displayed. A concept diagram of the dynamic pain connectome is also shown. Red indicates ascending nociceptive pathway, blue indicates the descending anti-nociceptive pathway, yellow indicates the default mode network and green indicates the salience network. AI, anterior insula; MCC, midcingulate cortex; mPFC, medial prefrontal cortex; NP, neuropathic pain; NNP, non-neuropathic pain; PCC, posterior cingulate cortex; PI, posterior insula; sgACC, subgenual anterior cingulate cortex; S1, primary somatosensory cortex; S2, secondary somatosensory cortex; TH, thalamus; TPJ, temporoparietal junction.

dynamic functional coupling abnormalities within the dynamic pain connectome. The neuropathic group had reduced cross-network dynamic amplitude envelope correlation between Asc-SN (left posterior insula-right TPJ, $p = 0.006$) (Fig. 4b) in the theta band. There was also abnormal cross-network dynamic wPLI between Asc-SN (right thalamus-right TPJ, $p = 0.009$) in the theta band (Fig. 4b), Desc-DMN (subgenual ACC-mPFC, $p = 0.001$) in the beta band and SN-DMN

(MCC-mPFC, $p = 0.009$) in the alpha band.

3.6. Subgroup analysis: abnormal functional coupling in non-neuropathic pain

The non-neuropathic pain group had reduced static amplitude envelope correlation between inter-hemispheric nodes of the ascending
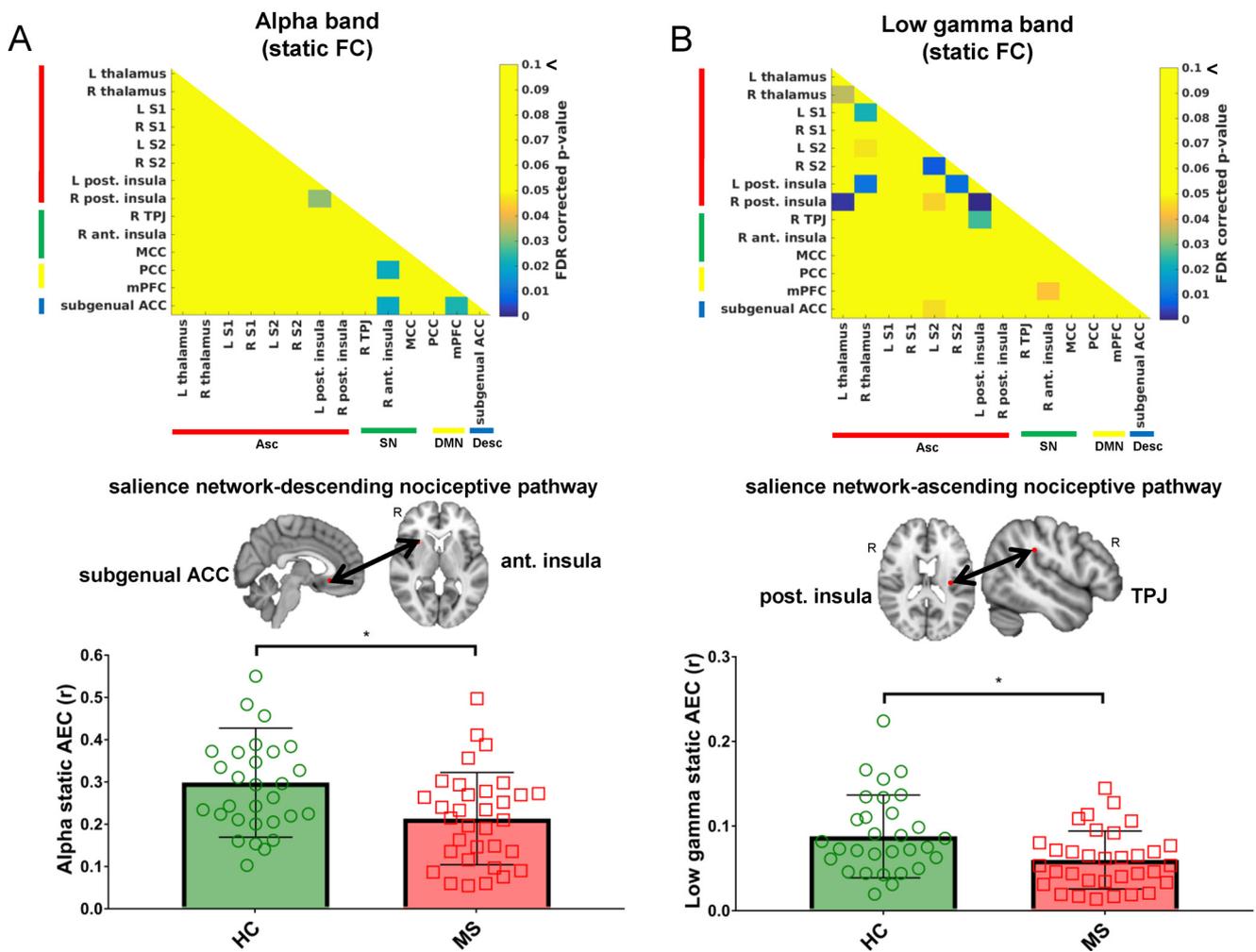
Fig. 2. Whole group comparison of static functional coupling between the healthy control (HC) group (green) and the multiple sclerosis (MS) chronic pain group (red).

Matrices indicate significant group differences for the alpha (A) and low gamma band (B). Examples of static functional coupling for the HC and MS groups based on amplitude envelope coupling are shown in the bar groups with symbols indicating individual participants and lines indicating means ± standard deviation. Significance set at $p < 0.05$ with FDR correction. ACC, anterior cingulate cortex; AEC, amplitude envelope correlation; Ant. Insula, anterior insula; Asc, ascending nociceptive pathway; Desc, descending anti-nociceptive pathway; DMN, default mode network; FDR, false discovery rate; MCC, mid cingulate cortex; PCC, posterior cingulate cortex; post. Insula, posterior insula; S1, primary somatosensory cortex; S2, secondary somatosensory cortex; SN, salience network; TPJ, temporoparietal junction.

nociceptive pathway, (right thalamus-left S2, $p = 0.002$) (Fig. 5a), (right S2-left S2, $p = 0.015$, $p = 0.003$) in the beta and low gamma bands. The non-neuropathic group also had decreased static amplitude envelope correlation between DMN-Desc (mPFC-subgenual ACC) in the alpha ($p = 0.009$) (Fig. 5a) and theta ($p = 0.008$) bands. In both the neuropathic and non-neuropathic groups, there was reduced static amplitude envelope correlation between inter hemispheric nodes of the ascending nociceptive pathway (left and right posterior insula, $p = 0.002$ (neuropathic), $p = 0.008$ (non-neuropathic)) in the low gamma band.

The non-neuropathic group had reduced dynamic amplitude envelope correlation in several cross-network nodes: SN-DMN (right anterior insula-PCC, $p = 0.0017$ and right anterior insula-mPFC, $p = 0.0018$) (Fig. 5b), Asc-SN (right S1-right anterior insula, $p = 0.008$ and right S1-MCC, $p = 0.01$) in the alpha band and Asc-DMN (right posterior insula-PCC, $p = 0.004$) in the beta band. The non-neuropathic group also had reduced dynamic wPLI within the DMN (PCC-mPFC, $p = 0.007$) in the theta band. All of these results are summarized in Fig. 1 and on Supplementary Tables 2 and 3.

3.7. Relationships between pain interference and pain severity with functional coupling of the dynamic pain connectome

We next examined the relationship between the functional coupling values which showed abnormalities and pain interference.

In the entire chronic pain group, within network static amplitude envelope correlation was negatively correlated with pain interference within inter-hemispheric nodes of the ascending nociceptive pathway (right thalamus-left S1) (rho = −0.35) (Fig. 6) in the beta band. Additionally, state pain was positively correlated with cross-network dynamic amplitude envelope correlation between nodes of the SN-DMN (right anterior insula-mPFC) (rho = 0.38) in the alpha band. State pain was also negatively correlated with cross-network static amplitude envelope correlation between nodes of the Asc-SN (left posterior insula-right TPJ) (rho = - 0.34) in the low gamma band. Finally, state pain was negatively correlated with within-network static amplitude envelope correlation between inter-hemispheric insula (rho = −0.36) in the low gamma band and between right thalamus-left S1 (rho = −0.47) in the beta band (Fig. 6).

In the neuropathic pain group, state pain was negatively correlated with abnormal within-network static amplitude envelope correlation of
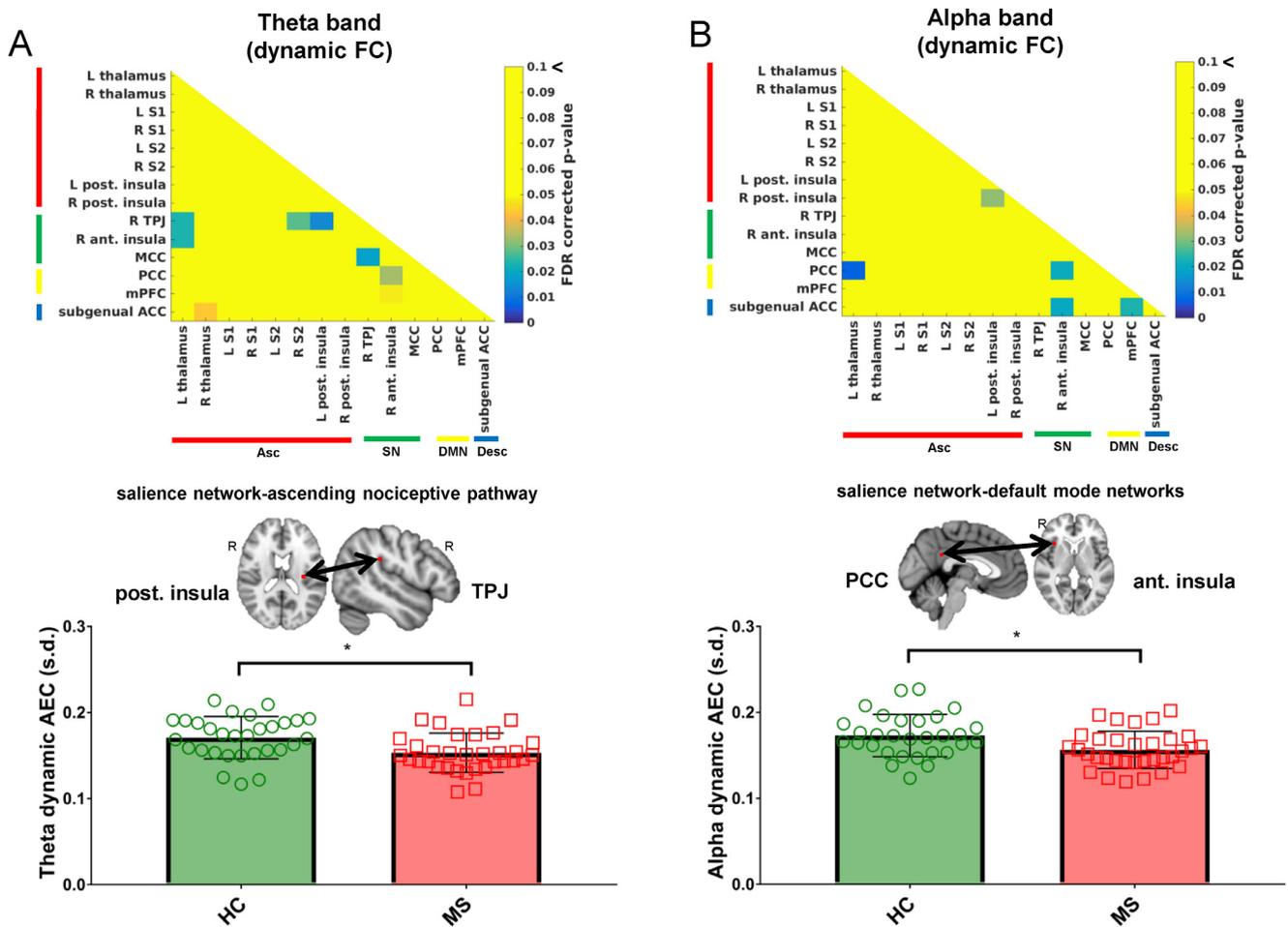
Fig. 3. Whole group comparison of dynamic functional coupling between the healthy control (HC) group (green) and the chronic pain multiple sclerosis (MS) group (red).
Matrices indicate significant group differences for the theta band (A) and alpha band (B). Examples of dynamic functional coupling for the HC and MS groups based on amplitude envelope coupling are shown in the bar groups with symbols indicating individual participants and lines indicating means ± standard deviation. Significance set at $p < 0.05$ with FDR correction. ACC, anterior cingulate cortex; AEC, amplitude envelope correlation; Asc, ascending nociceptive pathway; Desc, descending anti-nociceptive pathway; DMN, default mode network; FDR, false discovery rate; MCC, mid cingulate cortex; PCC, posterior cingulate cortex; S1, primary somatosensory cortex; S2, secondary somatosensory cortex; SN, salience network; TPJ, temporoparietal junction.

the ascending nociceptive pathway between the inter-hemispheric nodes of the posterior insula (rho $= -59$) (Fig. 6) in the low gamma band.

In the non-neuropathic pain group, cross-network dynamic amplitude envelope correlation was negatively correlated with pain interference between Asc-SN (right S1-right anterior insula) (rho $= -0.59$) (Fig. 6) in the alpha band. Furthermore, both trait pain and state pain were negatively correlated with cross-network dynamic amplitude envelope correlation between Asc-SN (right S1-right anterior insula) (rho $= -0.55$; rho $= -0.5$) (Fig. 6) in the alpha band.

4. Discussion

In this study, we demonstrated that patients with MS-related chronic pain exhibit aberrant broadband communication within and between brain networks of the dynamic pain connectome. These abnormalities impacted both static and dynamic FCp metrics identified using MEG. We also observed that some specific abnormalities were related to neuropathic pain versus non-neuropathic pain.

Fig. 1 highlights our main findings, first, patients with MS-related chronic pain exhibit pronounced altered FCp of the dynamic pain connectome. These abnormalities can be summarized as having four main features: a) specific temporal characteristics (broadband), b)

observed in both static and dynamic FCp, c) located across nodes of the salience network and the ascending nociceptive pathway, and d) observed both within- and across-networks. From our previous study on the same set of patients, the salience and ascending nociceptive pathway were two of the networks exhibiting the most pronounced regional abnormalities in chronic pain (Kim et al., 2019), demonstrating a possible link between regional and inter-regional abnormalities in chronic pain. Secondly, we found distinct static and dynamic FCp abnormalities that are present in the neuropathic and non-neuropathic pain groups across the dynamic pain connectome. This was an unexpected finding given our *a priori* hypothesis that abnormalities would be mostly pronounced in patients with neuropathic pain based on our previous regional study (Kim et al., 2019). Thus our study indicates that there are specific network abnormalities associated with neuropathic pain and with non-neuropathic chronic pain.

A prominent finding from this study was that our patients with MS related chronic pain exhibited cross-network FCp abnormalities. We and others have observed cross-network functional connectivity abnormalities in many chronic pain studies based on slow hemodynamics of fMRI (Baliki et al., 2008; Hemington et al., 2016; Bosma et al., 2018b, 2018a; Hemington et al., 2018; Rogachov et al., 2019). These studies are based on fMRI which provides limited temporal resolution and an indirect measure of neuronal activity. In the current study, we
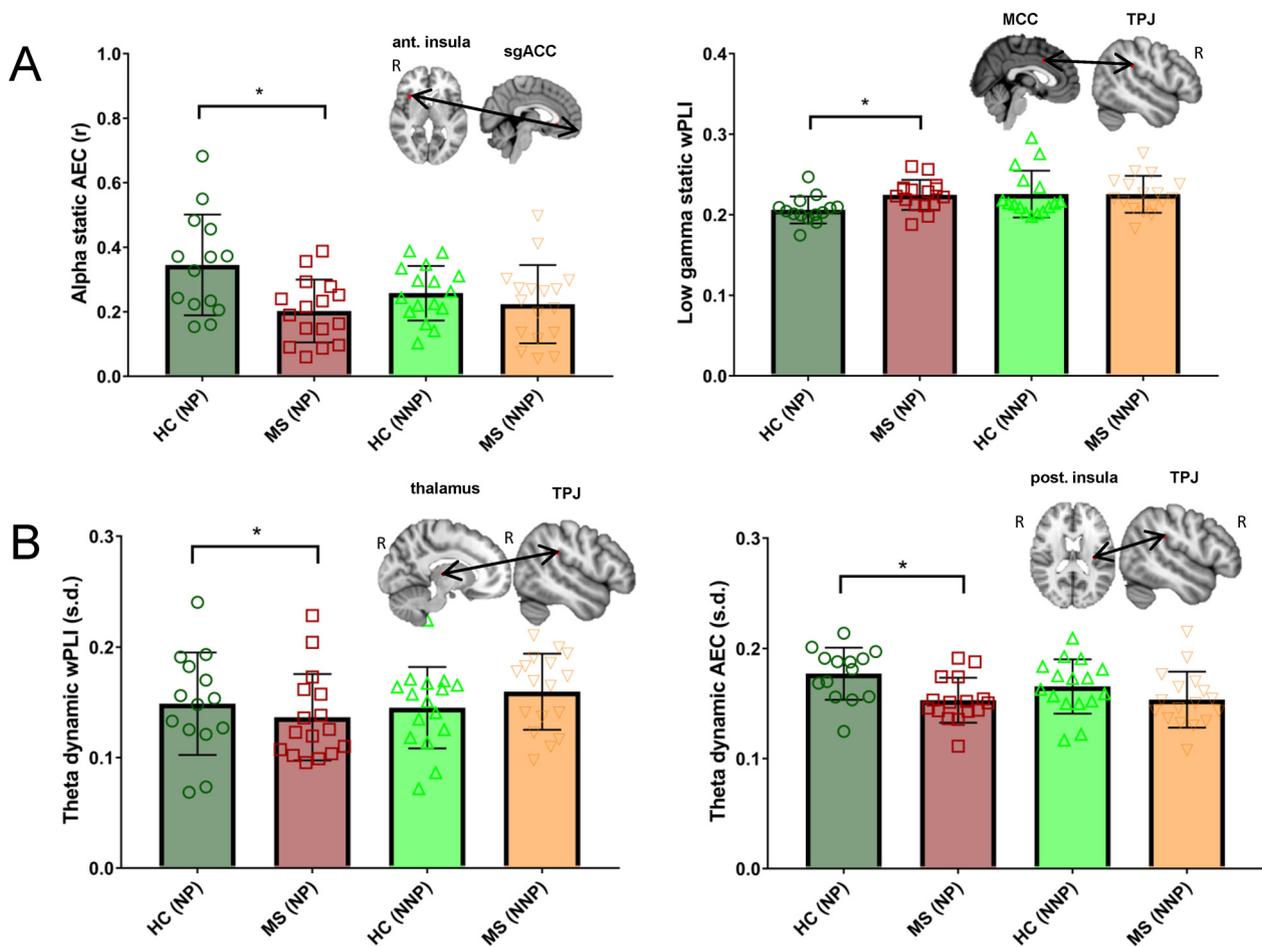
Fig. 4. Sub-group static and dynamic functional coupling comparison between NP and NNP and the matched HC.

All values are graphed as mean ± *S*.D. A) abnormal static functional coupling between salience network-descending anti-nociceptive pathway and within the salience network in NP B) abnormal cross-network dynamic functional coupling between salience network-ascending nociceptive pathway in NP. Significant differences at *p* < 0.05 with FDR correction. AEC, amplitude envelope correlation; HC, healthy control; NP, neuropathic pain; NNP, non-neuropathic pain; wPLI, weighted phase lag index.

have addressed some of these issues by utilizing MEG, which allows us to better investigate the fine temporal dynamics of cross-network abnormalities. The most prominent abnormalities from the study were observed in both static and dynamic FCp across SN-Asc nodes. SN-Asc and SN-Desc functional connectivity abnormalities were observed in a previous fMRI study in MS related chronic pain (Bosma et al., 2018a). As such, this particular interaction between networks associated with attention and the network associated with input of nociceptive information may be a hallmark of chronic pain, especially neuropathic pain. In chronic pain patients with MS, there was decreased coupling between the SN and the Asc which signifies desynchronization of the two networks. This particular cross-network abnormality may be present in MS due to the nature of the disease. In MS, both pain and cognitive deficits including attention are common issues (Archibald CJ et al., 1994; Hadjimichael et al., 2007; Zwibel and Smrtka, 2011). As such, there may be a complex interaction between the two systems in MS related chronic pain where cognitive deficits are compounded in the presence of chronic pain. If validated in additional studies, this finding may have significant clinical implications as treating chronic pain may become an important strategy to manage cognitive dysfunction in clinical practice. The SN and Asc nodes were previously shown to have the most pronounced regional abnormalities in MS-related chronic pain (Kim et al., 2019). Therefore, it was also interesting that our current study identified cross-network abnormalities within the same networks and it was also correlated with pain-related measures. As such this study not only showed a link between regional and cross-regional

abnormalities, but also showed that the relation between brain abnormalities and pain measures are consistent between regional and cross regional abnormalities.

In this study, abnormalities in inter-regional communication were observed mostly in nodes of the salience network. The specific cross-network abnormalities that were correlated with pain measures included SN-Asc and SN-DMN. SN-DMN cross-network abnormalities have been observed in previous studies in other chronic pain populations (Hemington et al., 2016). Under healthy conditions, the SN and the DMN are anti-correlated (Fox et al., 2005; Fransson, 2005). However, in chronic pain, those networks were correlated rather than anti-correlated with each other. In the case of MEG based FCp, we observed that static amplitude envelope correlation was reduced in patients with chronic pain. This may be explained by a previous study which compared resting state networks of MEG compared to fMRI and found that resting state networks are correlated only in the beta band range (Brookes et al., 2011). Our findings were observed in the alpha band range which may explain the discrepancy between the findings from fMRI.

The dynamics of functional connectivity between brain regions (Hutchison et al., 2013) especially in relation to physiological measures, including pain (Kucyi et al., 2013; Bosma et al., 2018b) are being increasingly studied. Brain dynamics is centered on the concept that the brain is intrinsically dynamic (Pinneo, 1966; Ward et al., 2006) and thought to be critical to functional organization in the brain (Malsburg et al., 2010). In chronic pain, studies have shown
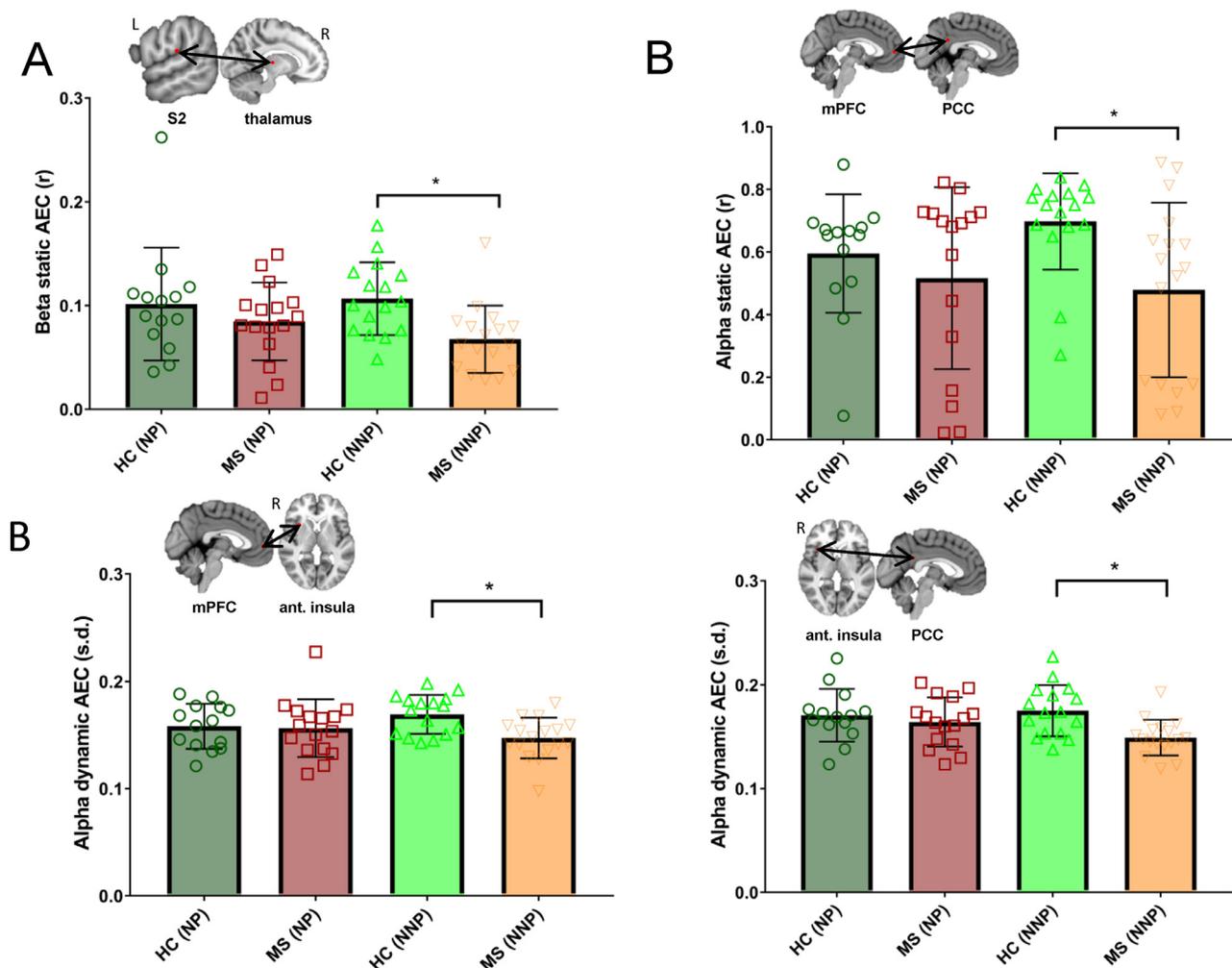
Fig. 5. Sub-group static and dynamic functional coupling comparison between NP and NNP and the matched HC.
All values are graphed as mean ± S.D. A) reduced within network ascending nociceptive pathway static amplitude envelope correlation in NNP compared to matched HC B) abnormal cross-network dynamic amplitude envelope correlation between salience network-default mode network in NNP. Significant differences at $p < 0.05$ with FDR correction. AEC, amplitude envelope correlation; HC, healthy control; NP, neuropathic pain; NNP, non-neuropathic pain; wPLI, weighted phase lag index.

abnormalities in dynamic functional connectivity in several chronic pain conditions including MS (Bosma et al., 2018b, 2018a; Rogachov et al., 2019). In particular, studies of patients with ankylosing spondylitis and MS have shown specific abnormalities in dynamic functional connectivity associated with neuropathic pain and in ankylosing spondylitis, different patterns of dynamic functional connectivity abnormalities were linked to their state and trait pain (Bosma et al., 2018b). In patients with MS, we have shown that dynamic FCp is attenuated across many cross-network nodes of the dynamic pain connectome. Reduction in dynamic FCp indicates that there is reduced flexibility in regional communication. Interestingly, we found reduced brain dynamics in both the neuropathic and non-neuropathic pain groups. This was in contrast to our expectations that we would observe abnormalities in neuropathic pain based on past chronic pains studies which showed pronounced abnormalities in neuropathic pain patients (Bosma et al., 2018b, 2018a). This suggests that the dynamic FCp abnormalities observed in the current study may be a general feature of chronic pain.

The use of MEG in the current study allowed us to examine coupling across different frequency bands. Abnormalities in FCp were observed in the theta, alpha, beta and low gamma bands. Among these, the alpha and beta bands have been implicated in pain processing in healthy controls (Ploner et al., 2006; Nir et al., 2012; Hu et al., 2013; Huishi Zhang et al., 2016; Furman et al., 2017). In patients with

neuropathic pain, resting state alpha power has previously been found to be abnormal, with a "slowing" of the alpha peak (Sarnthein et al., 2006; Stern et al., 2006; Cauda et al., 2010; Olesen et al., 2011; de Vries et al., 2013; Lim et al., 2016; Kim et al., 2019). Furthermore, abnormal theta-band power and coherence has been found in chronic pain conditions (Sarnthein and Jeanmonod, 2008; Leblanc et al., 2014). Therefore, there is evidence that theta, alpha, and beta may play specific roles in pain processing which is disrupted in chronic pain. We also found that gamma band activity is abnormal. In previous studies, gamma band activity has been inked with tonic pain ratings (Schulz et al., 2015). Experimental tonic pain is thought better reflect chronic pain because the stimulus is prolonged. Thus when gamma band activity was correlated with pain ratings in patients with chronic lower back pain, it was observed that gamma band activity was closely related to subjective pain ratings (May et al., 2019). While these studies focused on power, they showed that gamma oscillations may play an important role in pain processing especially in chronic conditions. Interestingly, we observed widespread gamma band FCp abnormalities both in within-and cross-network nodes and these abnormalities were correlated with trait and state pain. These results confirm the potential role of the gamma band in pain processing especially for chronic pain. The mechanism, however, is complex since the abnormalities were observed across multiple networks (Asc, SN, DMN). Taken together, these finding suggest that chronic pain may be a cumulative

Pain interference   Pain intensity
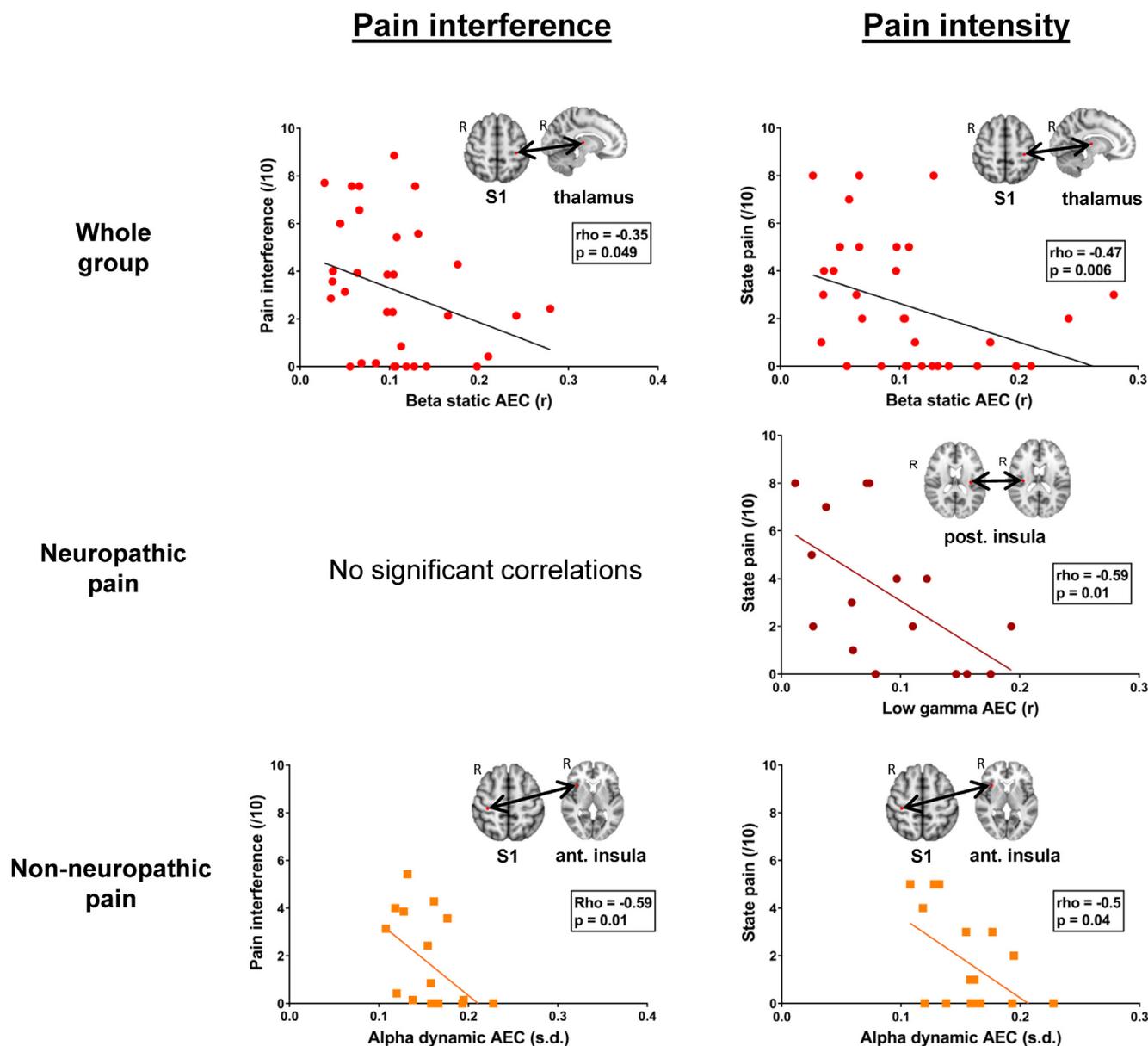
Fig. 6. Dynamic functional coupling correlated with pain interference and state pain.
Significant correlation observed between static/dynamic amplitude envelope correlation and pain interference in the whole chronic pain and non-neuropathic pain groups (left). Significant correlation observed between static/dynamic amplitude envelope correlation and state pain in the whole chronic group, neuropathic and non-neuropathic pain groups. AEC, amplitude envelope correlation.

consequence of gamma band asynchrony.

In conclusion, the current study revealed network level abnormalities in broadband communication within the dynamic pain connectome of people with chronic pain due to MS. Cross-network and within-network abnormalities were more pronounced within nodes that we previously found to exhibit regional abnormalities, demonstrating a link between regional and cross regional abnormalities. Furthermore, there were some commonalties and some specificity in the location and frequency band of aberrant coupling in neuropathic pain and non-neuropathic pain groups. These abnormalities were related with pain-specific measures such as pain severity and pain interference, suggesting a specific link to chronic pain in MS. Overall, the results of the study demonstrate cross-regional brain communication abnormalities specific to chronic pain in MS and abnormalities associated with neuropathic and non-neuropathic pain. A better understanding of the functional abnormalities underlying chronic pain in MS may eventually inform treatment strategies of this common and debilitating pain.

CRediT authorship contribution statement

Junseok A. Kim: Conceptualization, Data curation, Formal analysis, Methodology, Investigation, Project administration, Software, Visualization, Writing - original draft. **Rachael L. Bosma:** Investigation, Project administration, Writing - review & editing. **Kasey S. Hemington:** Investigation, Writing - review & editing. **Anton**

Rogachov: Investigation, Writing - review & editing. **Natalie R. Osborne:** Investigation, Writing - review & editing. **Joshua C. Cheng:** Investigation, Writing - review & editing. **Jiwon Oh:** Resources, Writing - review & editing. **Benjamin T. Dunkley:** Methodology, Writing - review & editing. **Karen D. Davis:** Conceptualization, Funding acquisition, Supervision, Writing - review & editing.

Declaration of Competing Interest

The authors have nothing to declare.

Acknowledgements

Supplementary materials

Supplementary material associated with this article can be found, in the online version, at doi:10.1016/j.nicl.2020.102230.

References

Archibald CJ, M.P., Ritvo, P.G., Fisk, J.D., Bhan, V., Maxner, C.E., Murray, T.J., 1994. Pain prevalence, severity and impact in a clinic sample of multiple sclerosis patients. Pain 58, 89–93.

Baliki, M.N., Geha, P.Y., Apkarian, A.V., Chialvo, D.R., 2008. Beyond feeling: chronic pain hurts the brain, disrupting the default-mode network dynamics. J Neurosci 28, 1398–1403.

Benjamini, Y., Hochberg, Y., 1995. Controlling the false discovery rate: a practical and powerful approach to multiple testing. Journal of the Royal Statistical Society Series B (Methodological) 57, 289–300.

Bosma, R.L., Kim, J.A., Cheng, J.C., Rogachov, A., Hemington, K.S., Osborne, N.R., Oh, J., Davis, K.D., 2018a. Dynamic pain connectome functional connectivity and oscillations reflect multiple sclerosis pain. Pain 159, 2267–2276.

Bosma, R.L., Cheng, J.C., Rogachov, A., Kim, J.A., Hemington, K.S., Osborne, N.R., Venkat Raghavan, L., Bhatia, A., Davis, K.D., 2018b. Brain dynamics and temporal summation of pain predicts neuropathic pain relief from ketamine infusion. Anesthesiology 129, 1015–1024.

Brookes, M.J., Woolrich, M., Luckhoo, H., Price, D., Hale, J.R., Stephenson, M.C., Barnes, G.R., Smith, S.M., Morris, P.G., 2011. Investigating the electrophysiological basis of resting state networks using magnetoencephalography. Proc Natl Acad Sci U S A 108, 16783–16788.

Buzsaki, G., 2006. Rhythms of the Brain. Oxford University Press.

Buzsáki, G., Draguhn, A., 2004. Neuronal oscillations in cortical networks. Science 304, 1926–1929.

Cauda, F., Sacco, K., Duca, S., Cocito, D., D'Agata, F., Geminiani, G.C., Canavero, S., 2009a. Altered resting state in diabetic neuropathic pain. PLoS ONE 4, e4542.

Cauda, F., Sacco, K., D'Agata, F., Duca, S., Cocito, D., Geminiani, G., Migliorati, F., Isoardo, G., 2009b. Low-frequency bold fluctuations demonstrate altered thalamo-cortical connectivity in diabetic neuropathic pain. BMC Neurosci 10, 138.

Cauda, F., D'Agata, F., Sacco, K., Duca, S., Cocito, D., Paolasso, I., Isoardo, G., Geminiani, G., 2010. Altered resting state attentional networks in diabetic neuropathic pain. J Neurol Neurosurg Psychiatry 81, 806–811.

Colclough, G.L., Brookes, M.J., Smith, S.M., Woolrich, M.W., 2015. A symmetric multivariate leakage correction for meg connectomes. Neuroimage 117, 439–448.

Davis, K.D., 2019. Imaging vs quantitative sensory testing to predict chronic pain treatment outcomes. Pain 160 (Suppl 1), S59–S65.

Davis, K.D., Cheng, J.C., 2019. Differentiating trait pain from state pain: a window into brain mechanisms underlying how we experience and cope with pain. Pain Reports 4, e735.

de Vries, M., Wilder-Smith, O.H., Jongsma, M.L., van den Broeke, E.N., Arns, M., van Goor, H., van Rijn, C.M., 2013. Altered resting state eeg in chronic pancreatitis patients: toward a marker for chronic pain. J Pain Res 6, 815–824.

Dworkin, R.H., et al., 2005. Core outcome measures for chronic pain clinical trials: impact recommendations. Pain 113, 9–19.

Fox, M.D., Snyder, A.Z., Vincent, J.L., Corbetta, M., Van Essen, D.C., Raichle, M.E., 2005. The human brain is intrinsically organized into dynamic, anticorrelated functional networks. Proc Natl Acad Sci U S A 102, 9673–9678.

Fransson, P., 2005. Spontaneous low-frequency bold signal fluctuations: an fMRI investigation of the resting-state default mode of brain function hypothesis. Hum Brain Mapp 26, 15–29.

Freynhagen, R., Baron, R., Gockel, U., Tolle, T.R., 2006. painDETECT: a new screening questionnaire to identify neuropathic components in patients with back pain. Curr Med Res Opin 22, 1911–1920.

Furman, A.J., Meeker, T.J., Rietschel, J.C., Yoo, S., Muthulingam, J., Prokhorenko, M., Keaser, M.L., Goodman, R.N., Mazaheri, A., Seminowicz, D.A., 2017. Cerebral peak alpha frequency predicts individual differences in pain sensitivity. Neuroimage 167, 203–210.

Goldenberg, M.M., 2012. Multiple sclerosis review. Pharmacy and Therapeutics 37, 175–184.

Hadjimichael, O., Kerns, R.D., Rizzo, M.A., Cutter, G., Vollmer, T., 2007. Persistent pain and uncomfortable sensations in persons with multiple sclerosis. Pain 127, 35–41.

Hemington, K.S., Wu, Q., Kucyi, A., Inman, R.D., Davis, K.D., 2016. Abnormal cross-network functional connectivity in chronic pain and its association with clinical symptoms. Brain Struct Funct 221, 4203–4219.

Hemington, K.S., Rogachov, A., Cheng, J.C., Bosma, R.L., Kim, J.A., Osborne, N.R., Inman, R.D., Davis, K.D., 2018. Patients with chronic pain exhibit a complex relationship triad between pain, resilience, and within- and cross-network functional connectivity of the default mode network. Pain 159, 1621–1630.

Hillebrand, A., Barnes, G.R., Bosboom, J.L., Berendse, H.W., Stam, C.J., 2012. Frequency-dependent functional connectivity within resting-state networks: an atlas-based meg beamformer solution. Neuroimage 59, 3909–3921.

Hu, L., Peng, W., Valentini, E., Zhang, Z., Hu, Y., 2013. Functional features of nociceptive-induced suppression of alpha band electroencephalographic oscillations. J Pain 14, 89–99.

Huishi Zhang, C., Sohrabpour, A., Lu, Y., He, B., 2016. Spectral and spatial changes of brain rhythmic activity in response to the sustained thermal pain stimulation. Hum Brain Mapp 37, 2976–2991.

Hutchison, R.M., Womelsdorf, T., Allen, E.A., Bandettini, P.A., Calhoun, V.D., Corbetta, M., Della Penna, S., Duyn, J.H., Glover, G.H., Gonzalez-Castillo, J., Handwerker, D.A., Keilholz, S., Kiviniemi, V., Leopold, D.A., de Pasquale, F., Sporns, O., Walter, M., Chang, C., 2013. Dynamic functional connectivity: promise, issues, and interpretations. Neuroimage 80, 360–378.

Jensen, T.S., Baron, R., Haanpaa, M., Kalso, E., Loeser, J.D., Rice, A.S., Treede, R.D., 2011. A new definition of neuropathic pain. Pain 152, 2204–2205.

Kim, J.A., Bosma, R.L., Hemington, K.S., Rogachov, A., Osborne, N.R., Cheng, J.C., Oh, J., Crawley, A.P., Dunkley, B.T., Davis, K.D., 2019. Neuropathic pain and pain interference are linked to alpha-band slowing and reduced beta-band magnetoencephalography activity within the dynamic pain connectome in patients with multiple sclerosis. Pain 160, 187–197.

Kucyi, A., Davis, K.D., 2015. The dynamic pain connectome. Trends Neurosci. 38, 86–95.

Kucyi, A., Davis, K.D., 2017. The neural code for pain: from single-cell electrophysiology to the dynamic pain connectome. Neuroscientist 23, 397–414.

Kucyi, A., Salomons, T.V., Davis, K.D., 2013. Mind wandering away from pain dynamically engages antinociceptive and default mode brain networks. Proc Natl Acad Sci U S A 110, 18692–18697.

Kurtzke, J.F., 1983. Rating neurologic impairment in multiple sclerosis: an expanded disability status scale (EDSS). Neurology 33, 1444–1452.

Leblanc, B.W., Lii, T.R., Silverman, A.E., Alleyne, R.T., Saab, C.Y., 2014. Cortical theta is increased while thalamocortical coherence is decreased in rat models of acute and chronic pain. Pain 155, 773–782.

Lim, M., Kim, J.S., Kim, D.J., Chung, C.K., 2016. Increased Low- and High-Frequency oscillatory activity in the prefrontal cortex of fibromyalgia patients. Front Hum Neurosci 10, 111.

Liu, Z., Fukunaga, M., de Zwart, J.A., Duyn, J.H., 2010. Large-scale spontaneous fluctuations and correlations in brain electrical activity observed with magnetoencephalography. Neuroimage 51, 102–111.

Llinas, R.R., Ribary, U., Jeanmonod, D., Kronberg, E., Mitra, P.P., 1999. Thalamocortical dysrhythmia: a neurological and neuropsychiatric syndrome characterized by magnetoencephalography. Proc Natl Acad Sci U S A 96, 15222–15227.

Malsburg, Cvd, Singer, W., Phillips, W.A., 2010. Dynamic Coordination in the brain: from Neurons to Mind. MIT Press, Cambridge, Mass.

May, E.S., Nickel, M.M., Ta Dinh, S., Tiemann, L., Heitmann, H., Voth, I., Tolle, T.R., Gross, J., Ploner, M., 2019. Prefrontal gamma oscillations reflect ongoing pain intensity in chronic back pain patients. Hum Brain Mapp 40, 293–305.

Melzack, R., 1975. The mcgill pain questionnaire: major properties and scoring methods. Pain 1, 277–299.

Melzack, R., Torgerson, W., 1971. On the language of pain. Anesthesiology 34, 50–59.

Nir, R.R., Sinai, A., Moont, R., Harari, E., Yarnitsky, D., 2012. Tonic pain and continuous EEG: prediction of subjective pain perception by alpha-1 power during stimulation and at rest. Clin Neurophysiol 123, 605–612.

O'Connor, A.B., Schwid, S.R., Herrmann, D.N., Markman, J.D., Dworkin, R.H., 2008. Pain associated with multiple sclerosis: systematic review and proposed classification. Pain 137, 96–111.

Olesen, S.S., Hansen, T.M., Graversen, C., Steimle, K., Wilder-Smith, O.H., Drewes, A.M., 2011. Slowed eeg rhythmicity in patients with chronic pancreatitis: evidence of abnormal cerebral pain processing? Eur J Gastroenterol Hepatol 23, 418–424.

Osborne, T.L., Raichle, K.A., Jensen, M.P., Ehde, D.M., Kraft, G., 2006. The reliability and validity of pain interference measures in persons with multiple sclerosis. J Pain Symptom Manage 32, 217–229.

Pinneo, L.R., 1966. On noise in the nervous system. Psychol Rev 73, 242–247.

Ploner, M., Gross, J., Timmermann, L., Pollok, B., Schnitzler, A., 2006. Pain suppresses spontaneous brain rhythms. Cereb Cortex 16, 537–540.

Rogachov, A., Bhatia, A., Cheng, J.C., Bosma, R.L., Kim, J.A., Osborne, N.R., Hemington, K.S., Venkatraghavan, L., Davis, K.D., 2019. Plasticity in the dynamic pain connectome associated with ketamine-induced neuropathic pain relief. Pain 160, 1670–1679.

Sarnthein, J., Jeanmonod, D., 2008. High thalamocortical theta coherence in patients with neurogenic pain. Neuroimage 39, 1910–1917.

Sarnthein, J., Stern, J., Aufenberg, C., Rousson, V., Jeanmonod, D., 2006. Increased eeg

power and slowed dominant frequency in patients with neurogenic pain. Brain: a journal of neurology 129, 55–64.

Schulz, E., May, E.S., Postorino, M., Tiemann, L., Nickel, M.M., Witkovsky, V., Schmidt, P., Gross, J., Ploner, M., 2015. Prefrontal gamma oscillations encode tonic pain in humans. Cereb Cortex 25, 4407–4414.

Siegel, M., Donner, T.H., Engel, A.K., 2012. Spectral fingerprints of large-scale neuronal interactions. Nat Rev Neurosci 13, 121–134.

Stern, J., Jeanmonod, D., Sarnthein, J., 2006. Persistent eeg overactivation in the cortical pain matrix of neurogenic pain patients. Neuroimage 31, 721–731.

Turk, D.C., et al., 2003. Core outcome domains for chronic pain clinical trials: immpact recommendations. Pain 106, 337–345.

Van Veen, B.D., van Drongelen, W., Yuchtman, M., Suzuki, A., 1997. Localization of brain electrical activity via linearly constrained minimum variance spatial filtering. IEEE Trans Biomed Eng 44, 867–880.

Vinck, M., Oostenveld, R., van Wingerden, M., Battaglia, F., Pennartz, C.M., 2011. An improved index of phase-synchronization for electrophysiological data in the presence of volume-conduction, noise and sample-size bias. Neuroimage 55, 1548–1565.

Walton, K.D., Dubois, M., Llinas, R.R., 2010. Abnormal thalamocortical activity in patients with complex regional pain syndrome (CRPS) type i. Pain 150, 41–51.

Ward, L.M., Doesburg, S.M., Kitajo, K., MacLean, S.E., Roggeveen, A.B., 2006. Neural synchrony in stochastic resonance, attention, and consciousness. Can J Exp Psychol 60, 319–326.

Zigmond, A.S., Snaith, R.P., 1983. The hospital anxiety and depression scale. Acta Psychiatr Scand 67, 361–370.

Zwibel, H.L., Smrtka, J., 2011. Improving quality of life in multiple sclerosis: an unmet need. Am J Manag Care 17 (Suppl 5 Improving) S139-145.